Reprinted from Journal of the Optical Society of America A, Vol. 4, page 1407, August 1987


# Polarization parameters of plane waves in hybrid birefringent optical fibers

**Charles Y. H. Tsao**

*Optical Fibre Group, Department of Electronics and Computer Science, University of Southampton, Southampton SO9 5NH, UK*

Received July 21, 1986; accepted December 1, 1986

The formulas determining the polarization ellipse from a given electric field's components and vice versa are summarized. The objective of this paper is then to study the polarization evolution (plane-wave evolution) in a curvilinear optical fiber with both linear and circular birefringence. As a result, the Jones-matrix–coupled-mode description has been extended to cover a fiber with distributed principal axes and linear and circular birefringence, and the plane-wave components of the emerging output light are conveniently quantified in terms of the input light. The detailed procedure of this extension is discussed through the use of the field's continuity, and the formulism is applied exclusively to various fibers such as twisted or spun and helical or spiral fibers of varying twist ratios, which may already have experienced external optical activity (side pressure, magnetic or electric fields, etc.). The conclusion drawn through this extended matrix technique is usually in good agreement with a range of the existing theoretical analyses (for evenly twisted fibers) and experimental results (for helical or spiral fibers, magnetic sensors, etc.), yet the approach proposed here obviously deals with a more general case and should therefore prove useful in practice.

## INTRODUCTION

Polarization properties have long been useful in describing optical devices such as linear or circular retarders and polarizers. While the status of a polarization ellipse (ellipticity and inclined angle) may be conveniently mapped onto the traditional Poincaré sphere, the vector descriptions (e.g., Stokes and Jones vectors) together with the relevant calculi (Mueller and Jones calculus) have been revised to describe the field components of polarized light.[1-5] These calculi are useful short-cut techniques and have formed the basis for a more general matrix and/or matrix-operator analysis, which has already proved useful in paraxial optics.[6-9] Optical fibers may be modeled as a particular type of optical device, and the polarization properties are often important, although the fiber may not be treated paraxially. For instance, high- and low-birefringence fibers,[10] fiber sensors,[11-15] and spun or twisted fibers[16-18] are of hybrid birefringence in nature, and the polarization fields are obviously coupled. For these optical fibers there are several techniques available, such as the field coupling approach[16-18] (which is essentially a differentiation description), the eigenpolarization mode method,[19] the equivalence of the combination of linear retarder $R$–principal axis $\Phi$–circular retarder $\Omega$ (R–$\Phi$–$\Omega$ equivalence) description,[20,21] and the group-theory formalism.[22] The eigenpolarization mode description (in which no mode coupling is present) usually relies on the coupled-mode formalism, which is essentially an extension of the decoupled differentiation approach. The R–$\Phi$–$\Omega$ equivalence method seems quite successful in handling optical devices that have lumped birefringence but has not yet been proved efficient in the treatment of fibers having distributed hybrid birefringence since in this case the R–$\Phi$–$\Omega$ matrix is not always commutative.[21] The group-theory formalism turns out to be a unified method and can indeed provide much useful insight into the overall behavior of the fiber matrix, yet a detailed description of the polarization cannot be readily obtained without knowledge of the structure of the individual fiber. The merit of this pure mathematical formalism is therefore rather restricted. The coupled-mode approach is the most useful of these techniques for a group of fibers such as spun or twisted fibers and might be extended to handle fibers that have a varying twist ratio and/or distributed linear birefringence. In recent years, however, many novel combinations of linear and circular birefringence have been common, and practical fibers such as helical and spiral fibers have exhibited complexity in terms of optical axes and the polarization couplings.[23-28] Besides, a fiber may often be exposed to an environment in which the optical activity or the state of the polarization in some region of the fiber is under the influence of an external magnetic or electric field, resulting in Faraday–Kerr effects.

Mechanical handling owing to pressing and bending may also affect the state of polarization.[11-14,21,24,27] Under these circumstances birefringence is often hybrid and distributed, in which case the coupling-differentiation description can hardly be straightforward. An alternative analysis is obviously desired. One possibility for such a technique is explored in this paper.

The method proposed here is the extension of the Jones calculus in which the importance of the field components is represented by a Jones vector, for plane waves propagating in a fiber in which hybrid birefringence is dominant. The technique adopted in this paper is quite reasonable in that it can provide sufficient information about the field components, which in turn determines uniquely the polarization properties of the light emerging from the end face of a curvilinear fiber. The mathematics using this matrix algorithm is usually straightforward for twisted or helically wound fibers that may be also exposed to a magnetic field. Some applications are presented. This procedure is obviously useful even for optical devices that may not be paraxial.

0740-3232/87/081407-06$02.00 

## FIELD COMPONENTS AND POLARIZATION ELLIPSE

Phase and amplitude information of an electric field can be used to determine uniquely the polarization ellipse. The eccentricity $e$, the ratio of the minor axis over the major axis of the polarization ellipse (see Fig. 1), and the inclined angle $\phi$ are related to the electric field in the following way:

$$\tan 2\phi = 2\,\mathrm{Re}(E_x E_y^*)/(|E_x|^2 - |E_y|^2), \tag{1a}$$

$$e = \tan\{\tfrac{1}{2}\sin^{-1}[2\,\mathrm{Im}(E_x^* E_y)/(|E_x|^2 + |E_y|^2)]\}, \tag{1b}$$

where $E_x$ and $E_y$ are the $x$ and $y$ components of the Jones vector $\begin{bmatrix} E_x \\ E_y \end{bmatrix}$ and the asterisk indicates the complex conjugate. Strictly speaking, the field must involve the factor $e^{j(\omega t - \bar{\beta}s)}$, where $\omega$ is the circular frequency of the light, $\bar{\beta}$ is the mean propagation constant, and $s$ is the distance along the light path. This factor is usually irrelevant to the polarization ellipse and is often neglected. However, the detailed description of the ellipse given in Eqs. (1) does not determine uniquely the field's components $E_x$ and $E_y$, and alternatively the normalized electric field components may be utilized. The normalization Jones vector then takes the form of $\begin{bmatrix} 1 \\ \rho e^{j\epsilon} \end{bmatrix}$ or $\begin{bmatrix} e^{-j\epsilon}/\rho \\ 1 \end{bmatrix}$ ($\rho = |E_y/E_x|$, $\epsilon = \arg E_y - \arg E_x$) for which the polarization ellipse may be described by Eqs. (2):

$$\tan\phi = \frac{\rho\cos(\Omega_m + \epsilon)}{\cos\Omega_m}, \tag{2a}$$

$$e^2 = \frac{\tan^2\phi - \rho^2}{\rho^2\tan^2\phi - 1}, \tag{2b}$$

$$P_e = \frac{1 - e^2}{1 + e^2} = \frac{(1 - \rho^2)[\tan^2\epsilon + (1 + \rho^2)/(1 - \rho^2)]^{1/2}}{(1 + \rho^2)(\tan^2\epsilon + 1)^{1/2}}, \tag{2c}$$

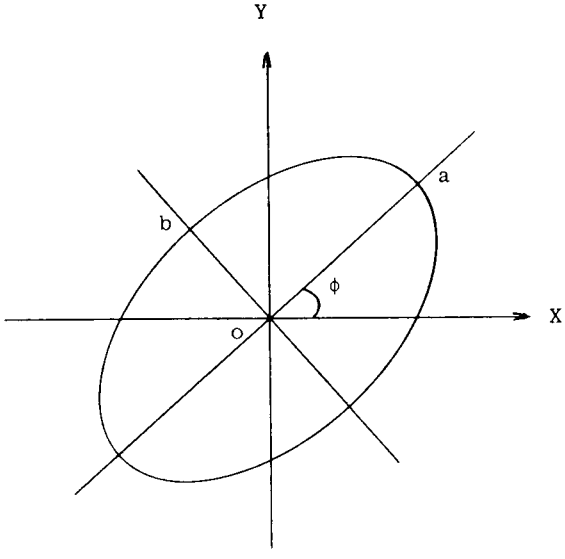


Fig. 1. The polarized ellipse in $X$–$Y$ coordinates.

$$\Omega_m = \tfrac{1}{2}\tan^{-1}\left(\frac{-\rho^2\sin 2\epsilon}{1 + \rho^2\cos 2\epsilon}\right). \tag{2d}$$

Here the parameter $P_e$ defines the degree of the polarization and is sometimes termed the polarization ellipticity. The Jones vector normalized in this way can be determined uniquely from the polarization ellipse $(e, \phi)$ through Eqs. (3):

$$\rho = [(\tan^2\phi + e^2)/(e^2\tan^2\phi + 1)]^{1/2}, \tag{3a}$$

$$\epsilon = \sin^{-1}\{e(\tan^2\phi + 1)/[(e^2\tan^2\phi + 1)(\tan^2\phi + e^2)]^{1/2}\}, \tag{3b}$$

or

$$\epsilon = \cos^{-1}[(1 - e^2)\tan\phi/[(e^2\tan^2\phi + 1)(\tan^2\phi + e^2)]^{1/2}\}. \tag{3c}$$

## DISCRETE OPTICAL DEVICES

Suppose that light with $X$ and $Y$ components $\begin{bmatrix} E_x^i \\ E_y^i \end{bmatrix}$ is launched into a discrete optical device possessing linear and circular birefringence. Then the output $\begin{bmatrix} E_x^o \\ E_y^o \end{bmatrix}$ may be described by using a matrix notation:

$$\begin{bmatrix} E_x^o \\ E_y^o \end{bmatrix} = M_{lr}^{xy}\begin{bmatrix} E_x^i \\ E_y^i \end{bmatrix} \tag{4a}$$

or

$$\begin{bmatrix} E_x^o \\ E_y^o \end{bmatrix} = M_{rcr}^{xy}\begin{bmatrix} E_x^i \\ E_y^i \end{bmatrix}, \tag{4b}$$

where

$$M_{lr}^{xy} = \begin{Bmatrix} \exp(j\tfrac{1}{2}\delta_l)\cos^2\psi + \exp(-j\tfrac{1}{2}\delta_l)\sin^2\psi & [\exp(j\tfrac{1}{2}\delta_l) - \exp(-j\tfrac{1}{2}\delta_l)]\sin\psi\cos\psi \\ [\exp(j\tfrac{1}{2}\delta_l) - \exp(-j\tfrac{1}{2}\delta_l)]\sin\psi\cos\psi & \exp(j\tfrac{1}{2}\delta_l)\sin^2\psi + \exp(-j\tfrac{1}{2}\delta_l)\cos^2\psi \end{Bmatrix} \tag{4c}$$

and where

$$M_{rcr}^{xy} = \begin{bmatrix} \cos\tfrac{1}{2}\delta_c, & \sin\tfrac{1}{2}\delta_c \\ -\sin\tfrac{1}{2}\delta_c & \cos\tfrac{1}{2}\delta_c \end{bmatrix}. \tag{4d}$$

Here $\psi$ denotes the angle between the $X$ axis and the fast axis of the linear retarder, $\delta_l$ and $\delta_c$ are measures of linear and circular retardation, respectively, and the subscripts lr and rcr indicate linear retarder and right circular retarder, respectively. The matrices $M_{lr}^{xy}$ and $M_{rcr}^{xy}$ in Eqs. 4(c) and 4(d) are not necessarily unique, yet the formulation is sufficient to reveal the polarization properties of the light. If both linear and circular retardation is present within a device, the matrix representation remains valid, and the output light is described by

$$\begin{bmatrix} E_x^o \\ E_y^o \end{bmatrix} = M_{hlc}^{xy}\begin{bmatrix} E_x^i \\ E_y^i \end{bmatrix} \tag{4e}$$

or

$$\begin{bmatrix} E_x^o \\ E_y^o \end{bmatrix} = M_{hcl}^{xy}\begin{bmatrix} E_x^i \\ E_y^i \end{bmatrix}. \tag{4f}$$

Here $M_{hlc}^{xy} = M_{lr}^{xy} \times M_{rcr}^{xy}$, and $M_{hcl}^{xy} = M_{rcr}^{xy} \times M_{lr}^{xy}$, the choice of which depends on which retarder goes first, as the subscripts hcl/hlc imply. Care should be taken with this straightforward representation. Since $M_{hlc}^{xy} \neq M_{hcl}^{xy}$, the output light of the $X$–$Y$ components may correspond to different eigenstates and, therefore, to different polarization

ellipses even when the input light is identical. There are, however, cases in which the retardation order may not be so critical. For instance, if the principal optical axes $\xi$ and $\eta$, say, are taken as the $X$–$Y$ axes, then

$$M_{\mathrm{lr}}{}^{\xi\eta} = \begin{bmatrix} \exp(j\frac{1}{2}\delta_l) & 0 \\ 0 & \exp(-j\frac{1}{2}\delta_l) \end{bmatrix}, \tag{5a}$$

$$M_{\mathrm{rcr}}{}^{\xi\eta} = M_{\mathrm{rcr}}{}^{xy}, \tag{5b}$$

$$M_{\mathrm{hlc}}{}^{\xi\eta} = \begin{bmatrix} \exp(j\frac{1}{2}\delta_l)\cos\frac{1}{2}\delta_c & \exp(j\frac{1}{2}\delta_l)\sin\frac{1}{2}\delta_c \\ -\exp(-j\frac{1}{2}\delta_l)\sin\frac{1}{2}\delta_c & \exp(-j\frac{1}{2}\delta_l)\cos\frac{1}{2}\delta_c \end{bmatrix}, \tag{5c}$$

and

$$M_{\mathrm{hcl}}{}^{\xi\eta} = \begin{bmatrix} \exp(j\frac{1}{2}\delta_l)\cos\frac{1}{2}\delta_c & -\exp(-j\frac{1}{2}\delta_l)\sin\frac{1}{2}\delta_c \\ \exp(j\frac{1}{2}\delta_l)\sin\frac{1}{2}\delta_c & \exp(-j\frac{1}{2}\delta_l)\cos\frac{1}{2}\delta_c \end{bmatrix}. \tag{5d}$$

It is obvious from Eqs. (5c) and (5d) that in spite of the fact that $M_{\mathrm{hlc}}{}^{\xi\eta}$ and $M_{\mathrm{hcl}}{}^{\xi\eta}$ are not equal, they nevertheless correspond to the same eigenstates and can therefore represent the same polarization ellipse. In other words, as far as polarization is concerned, the order in which retardation occurs is not required to be clearly stated as long as the principal axes are taken as the field axes.

## THE OPTICAL FIBER

Let us now study the polarization behavior of the light propagating in an optical fiber in which linear and circular birefringence is distributed. One method of analysis is to describe the fiber with parameters distributed in this way as consisting of many infinitesimal segments, each of which is treated as an indepenent optical device. The light output from the last of these is then the light emerging from the end-face of the given fiber. This makes sense because, as we saw in the previous section, if the principal axes of each segment are taken as the field axes, then the order of the distributed linear and circular retardation in each segment is not important. Bearing this in mind, we shall first order these chopped pieces and then write the formula for the output light emerging from the last segment as

$$\begin{bmatrix} E_{\xi n} \\ E_{\eta n} \end{bmatrix} = \prod_{k=1}^{n} M_{\mathrm{lr}}{}^{k} M_{\mathrm{rcr}}{}^{k} M_{k-1}{}^{k} \begin{bmatrix} E_{\xi_0} \\ E_{\eta_0} \end{bmatrix}. \tag{6a}$$

Here the principal axes of the $k$th piece are $\xi k/\eta k$ ($\xi_0/\eta_0$ being the input field's components axes), $M_{\mathrm{lr}}{}^{\xi k\eta k}/M_{\mathrm{rcr}}{}^{\xi k\eta k}$ are abbreviated as $M_{\mathrm{lr}}{}^{k}/M_{\mathrm{rcr}}{}^{k}$, and $M_{k-1}{}^{k}$ is the rotation matrix converting the axes from $\xi(k-1)/\eta(k-1)$ to $\xi k/\eta k$. A straightforward calculation leads to

$$M_{\mathrm{lr}}{}^{k} M_{\mathrm{rcr}}{}^{k} M_{k-1}{}^{k} = \begin{bmatrix} \exp(j\frac{1}{2}\delta_l'\Delta s)\cos(\psi' + \frac{1}{2}\delta_c')\Delta s, & \exp(j\frac{1}{2}\delta_l'\Delta s)\sin(\psi' + \frac{1}{2}\delta_c')\Delta s \\ -\exp(-j\frac{1}{2}\delta_l'\Delta s)\sin(\psi' + \frac{1}{2}\delta_c')\Delta s, & \exp(-j\frac{1}{2}\delta_l'\Delta s)\cos(\psi' + \frac{1}{2}\delta_c')\Delta s \end{bmatrix} \tag{6b}$$

or

$$M_{\mathrm{lr}}{}^{k} M_{\mathrm{rcr}}{}^{k} M_{k-1}{}^{k} \approx I + M^{k}\Delta s, \tag{6c}$$

where

$$M^{k} = \begin{bmatrix} j\frac{1}{2}\delta_l', & \psi' + \frac{1}{2}\delta_c' \\ -(\psi' + \frac{1}{2}\delta_c'), & -j\frac{1}{2}\delta_l' \end{bmatrix} \tag{6d}$$

and where $\delta_l'$ and $\delta_c'$ are the ratios of the linear and circular retardations and the principal axis (twist, rotate) (i.e. the derivatives with respect to $s$: $\delta_l' = \mathrm{d}\delta_l/\mathrm{d}s$, $\delta_c' = \mathrm{d}\delta_c/\mathrm{d}s$, $\psi' = \mathrm{d}\psi/\mathrm{d}s$; $s$ is a measure along the fiber's length); and $I$ is the $2\times 2$ unit matrix. In the limit as $\Delta s \to 0$, $\xi n/\eta n$ and $E_{\xi v}/E_{\eta n}$ became the principal axes and the projected electric field observed at the endface of the fiber, which may be denoted as $\xi/\eta$ and $E_\xi{}^0/E_\eta{}^0$, respectively. On the other hand,

$$\lim_{\Delta s\to 0} \prod_{k=1}^{n} (I + M^{k}\Delta s) = M(s)$$

is a $2\times 2$ matrix that may be evaluated through the following relations:

$$M(s) = e^{A(s)},$$

$$A(s) = \begin{bmatrix} \lim\limits_{\Delta s\to 0} \sum\limits_{k=1}^{n} j\frac{1}{2}\delta_l'\Delta s, & \lim\limits_{\Delta s\to 0} \sum\limits_{k=1}^{n} (\psi' + \frac{1}{2}\delta_c')\Delta s \\ \lim\limits_{\Delta s\to 0} \sum\limits_{k=1}^{n} -(\psi' + \frac{1}{2}\delta_c')\Delta s, & \lim\limits_{\Delta s\to 0} \sum\limits_{k=1}^{n} -j\frac{1}{2}\delta_l'\Delta s \end{bmatrix}, \tag{6e}$$

or

$$A(s) = \begin{bmatrix} j\frac{1}{2}\delta_l(s), & \psi(s) + \frac{1}{2}\delta_c(s) \\ -\psi(s) - \frac{1}{2}\delta_c(s), & -j\frac{1}{2}\delta_l(s) \end{bmatrix}. \tag{6f}$$

The procedure for evaluating $M(s)$ from $A(s)$ is well known (Ref. 29, p. 124; Ref. 30, p. 121) and can easily be applied since $M(s)$ is the exponential of $A(s)$. According to this notation, the matrix function $F(A)$ is written as $\alpha + \beta A$, where $\alpha$ and $\beta$ are the coefficients determined by $F(\lambda_i) = \alpha + \beta\lambda_i$, of which $\lambda_i$ ($i = 1, 2$) are the eigenvalues of the matrix $A$. The eigenvalues of $A(s)$ in Eq. (6f) are $\pm j\lambda$, where $\lambda = [(\frac{1}{2}\delta_l)^2 + (\psi + \frac{1}{2}\delta_c)^2]^{1/2}$, so that $\alpha = \cos\lambda$ and $\beta = \sin\lambda/\lambda$. This implies that

$$\begin{bmatrix} E_\xi{}^0 \\ E_\eta{}^0 \end{bmatrix} = \begin{bmatrix} P(s) & -Q^*(s) \\ Q(s) & P^*(s) \end{bmatrix} \begin{bmatrix} E_\xi{}^i \\ E_\eta{}^i \end{bmatrix} \tag{7}$$

and

$$\begin{bmatrix} U_1{}^0 \\ U_2{}^0 \end{bmatrix} = \begin{bmatrix} e^{j\lambda} & 0 \\ 0 & e^{-j\lambda} \end{bmatrix} \begin{bmatrix} \xi_0{}^i + j(\Gamma - \sqrt{1+\Gamma^2})\eta_0{}^i \\ \xi_0{}^i - j(\Gamma + \sqrt{1+\Gamma^2})\eta_0{}^i \end{bmatrix}, \tag{7a}$$

$$P(s) = \cos\lambda + j\frac{\frac{1}{2}\delta_l}{\lambda}\sin\lambda, \tag{7b}$$

$$Q(s) = -\frac{(\psi + \frac{1}{2}\delta_c)}{\lambda}\sin\lambda, \tag{7c}$$

$$\Gamma(s) = \delta_l/(2\psi + \delta_c). \tag{7d}$$

Here $U_1{}^0$ and $U_2{}^0$ are the two output eigenstates and $\xi_0{}^i/\eta_0{}^i$ are the two unit vectors of the input axes. This is the field matrix that describes exactly how the state of polarization evolves along a fiber of hybrid birefringences and what the eigenstates are for any given length of the fiber. The formu-

la is remarkably simple and can be invoked to describe general curvilinear optical fibers such as twisted or spun and helical or spiral fibers.

## TWISTED AND SPUN FIBERS

Equations (7) describe exactly how a plane wave evolves in an optical fiber of varying hybrid birefringences. We now show that this extended Jones matrix formalism can be useful in the analysis of various individual curvilinear fibers. We begin with twisted or spun fibers of varying twist ratio $\psi' = \tau(s)$. The only difference between twisted and spun fibers is the presence of torsional stress in the twisted case. This, in turn, induces circular birefringence $\frac{1}{2}\delta_c' = -g\tau(s)$, where $g = 0.065 \sim 0.08$ is a constant determined by theory. It is in close agreement with experimental measurement.[14,15,17] The minus is due to the fact that the right-hand twist causes an $l$-rotary optical activity (left circular retardation). From the original definitions we obtain

$$\psi + \tfrac{1}{2}\delta_c = \int (1-g)\tau(s)\mathrm{d}s = (1-g)\bar{\tau}(s)s, \tag{8a}$$

$$\tfrac{1}{2}\delta_l = \int \tfrac{1}{2}\delta_l'(s)\mathrm{d}s = \tfrac{1}{2}\bar{\delta}_l'(s)s, \tag{8b}$$

$$\lambda = \bar{\lambda}'(s)s = [(\tfrac{1}{2}\bar{\delta}_l')^2 + (1-g)^2\bar{\tau}^2(s)]^{1/2}s, \tag{8c}$$

where $\bar{\tau}(s)$, $\bar{\delta}_l'(s)$, and $\bar{\lambda}'(s)$ are the averaged twist ratio, linear retardation, and eigenvalue, respectively. The output field in Eqs. (7) is expressed by Eqs. (8d) and (8e):

$$E_\xi^0 = (\cos\bar{\lambda}'s + j\frac{\frac{1}{2}\bar{\delta}_l'}{\bar{\lambda}}\sin\bar{\lambda}'s)E_\xi^i + \frac{(1-g)\bar{\tau}}{\bar{\lambda}}\sin\bar{\lambda}'sE_\eta^i, \tag{8d}$$

$$E_\xi^0 = -\frac{(1-g)\bar{\tau}}{\bar{\lambda}'}\sin\bar{\lambda}'sE_\xi^i + \left(\cos\bar{\lambda}'s - j\frac{\frac{1}{2}\bar{\delta}_l'}{\bar{\lambda}}\sin\bar{\lambda}'s\right)E_\eta^i. \tag{8e}$$

In the case when the fiber is modeled by an evenly distributed linear and circular birefringence/twist ratio, the parameters with the overbars in Eqs. (8) would be constant, and the above field appears to be the formulation derived in Refs. 11, 16, and 17. It is stressed that Eqs. (8) handle varying principal axes and hybrid birefringence. They are therefore more suitable for a range of applications in which the varying linear birefringence is possibly quenched by a varying twist. This should also apply to the case when there is immunity from external effects such as side pressure for a particular fiber. The basic technique so far is to average the relevant parameters over the fiber length. The output field then is still in a familiar matrix form, which seems useful even when the fiber is partially exposed to random disturbances.

## HELICAL FIBER

Suppose that a section of fiber is wound, without being twisted, into a helix of radius $R$ with pitch $p$ ($b = p/2\pi$) (see Fig. 2). Suppose further the fiber possesses a negligible intrinsic linear birefringence relative to a stress-induced birefringence. If this is not the case, or if twist is present, the

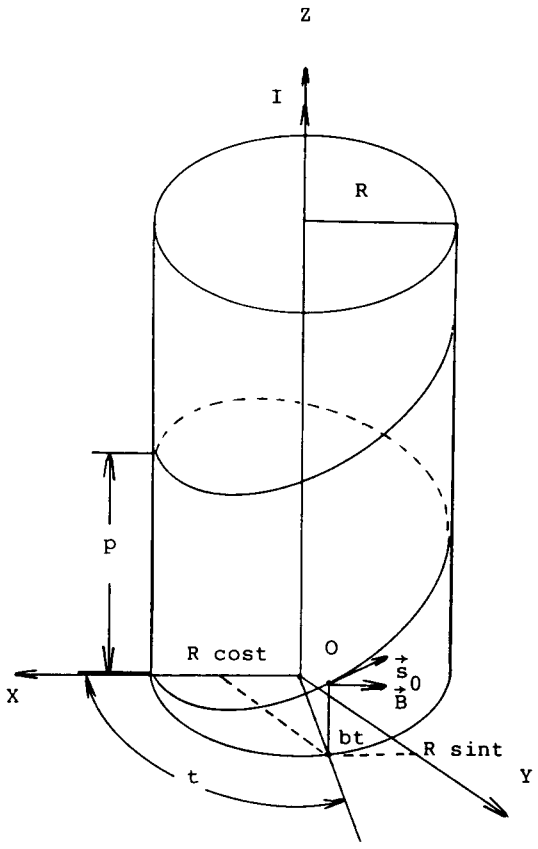


Fig. 2. A right-handed helical optical fiber.

determination of the overall birefringence and the principal axes is to be carried out before the following matrix-evaluation routine is applied. A typical magnitude of the bending-induced birefringence is given by $\delta_l' = 1.344 \times 10^6\,\chi^2 r^2$ rad/m, of which the binormal axis is the fast axis, $\chi = R/(R^2 + b^2)$ is the curvature, and $r$ is the fiber radius.[27] (The parameters $R$, $r$, $b$, $p$, and $s$ are given in meters.) From the helical geometry it is obvious that the normal and binormal axes, as defined in the Serret–Frenet formulas, rotate around the tangential vector at the rate of $\tau$, $\tau = \pm b/(R^2 + b^2)$. If the sign is positive, then the helix is right-handed, as shown in Fig. 2; otherwise it is left-handed.[31] It is also well known that the polarization ($HE_{11}$ modes) is observed in Tang's torsionless frame, and so the principal axis can be written in the form $\psi = \tau s$ since $\tau$ is a constant.[23,24,28] Under the assumption that no external optical activity is present, one obtains

$$\tfrac{1}{2}\delta_l = \tfrac{1}{2}\delta_l's,$$

$$\lambda = \frac{s}{(R^2+b^2)}\left[\left(0.672\times 10^6\frac{R^2r^2}{R^2+b^2}\right)^2 + (1-g)^2b^2\right]^{1/2}.$$

The output field is then easily established from Eqs. (7). We emphasize that if the fiber has low stress-induced birefringence, such as a liquid-core fiber does, then we may assume that $\frac{1}{2}\delta_l' = 0$ and $g = 0$. Then the output field is given by

$$\begin{bmatrix} E_\xi^0 \\ E_\eta^0 \end{bmatrix} = \begin{bmatrix} \cos\tau s & \sin\tau s \\ -\sin\tau s & \cos\tau s \end{bmatrix}\begin{bmatrix} E_\xi^i \\ E_\eta^i \end{bmatrix}. \tag{9}$$

This describes a $d$-rotatory polarization (right circular retarder), as indicated in Refs. 12 and 23. From our experimental work, this $d$-rotatory activity can also be measured in a stressed helix when the pitch length/radius ratio of the helix is reasonably large, such that $|0.672 \times 10^6 [R^2 r^2/b(R^2 + b^2)]| \ll 1$ is satisfied. Then the linear birefringence is automatically quenched by the principal axis rotation, again because of optical activity in Eq. (9), and becomes equal to $(1 - g)\tau$.

## HELICAL/SPIRAL FIBER WITHOUT EXTERNAL OPTICAL ACTIVITY

Stress-induced birefringence is usually much more significant than geometry-induced birefringence. The latter can often be neglected whenever the former is present. There are occasions, though, in which the stress is eliminated by means of an annealing or drawing process. Then geometry-induced birefringence may become evident. From an analysis using the vector-wave equation it has been shown that the amount of birefringence in a helical fiber of step-index profile (Fig. 3) is $\frac{1}{2}\delta_l' = (\chi^2 a^2 \beta/8V^2)(9W^2/U^2 - 7U^2/W^2)$, of which the normal axis defined in Tang's torsionless frame is the fast axis when $V > 1.372$, where $V = ka(n_{co}^2 - n_{cl}^2)^{1/2}$ is the normalized frequency. Here $a$ is the core radius, $k$ is the wave number in vacuum, $n_{co}$ and $n_{cl}$ are the core/clad refractive indices, and $\beta$ is the propagation constant. Also, $U = a(k^2 n_{co}^2 - \beta^2)^{1/2}$ and $W = a(\beta^2 - k^2 n_{cl}^2)^{1/2}$ are the core and cladding parameters, respectively.[28] Since the principal axes are the normal and the binormal of Tang's frame (here denoted as the $X$ and $Y$ axes), $\psi = 0$ and $\frac{1}{2}\delta_c = 0$, by definition. The output field in the $X$–$Y$ axes exhibits only a simple linear retardation, which can still be projected onto $\xi$ and $\eta$, the normal and binormal axes in the Serret–Frenet frame, as

$$\begin{bmatrix} E_\xi^{\,0} \\ E_\eta^{\,0} \end{bmatrix} = \begin{bmatrix} \exp(j\frac{1}{2}\delta_l' s)\cos\tau s & \exp(-j\frac{1}{2}\delta_l' s)\sin\tau s \\ -\exp(j\frac{1}{2}\delta_l' s)\sin\tau s & \exp(-j\frac{1}{2}\delta_l' s)\cos\tau s \end{bmatrix} \begin{bmatrix} E_\xi^{\,i} \\ E_\eta^{\,i} \end{bmatrix}. \tag{10}$$

The spiral fiber used in Ref. 26 is the type of the fiber discussed in this section. The fiber is characterized by $n_{co} = 1.46$, $n_{cl} = 1.45$, $V = 16.9$, $U = 2.26$, $W = 16.7$, $\chi^2 a^2 = 5.71 \times 10^{-8}$ rad (at the spiral twist rate 116 turns/m), $\beta = 1.449 \times 10^7$, $\tau s = 2\pi$ rad, and $\frac{1}{2}\delta_l' s = 2.006 \times 10^{-3}$ rad for each complete turn. According to Eq. (10) a close match should be expected between optical rotation and the spiral twist when a linearly polarized light is injected. This is exactly what has been measured in Ref. 26, in which the beat length corresponds to the half-pitch length, certainly for spiral twist rates no greater than 116 turns/m. This seems to be the maximum optical rotation measurable in that particular setup.

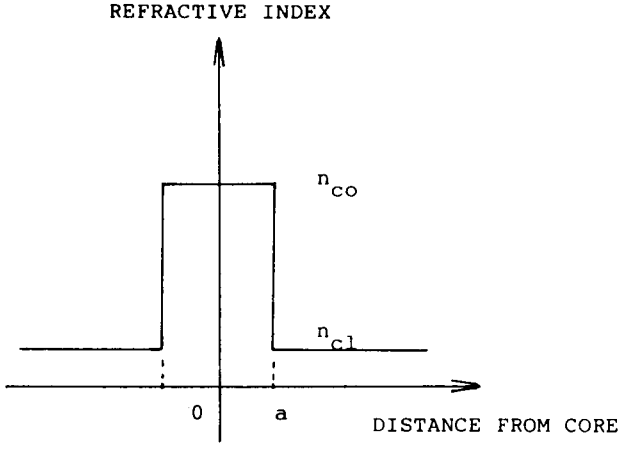


Fig. 3. The refractive-index profile of a helical fiber.

## HELIX EXPOSED TO AN EXTERNAL MAGNETIC FIELD

Since helical fiber might be useful as a current sensor, the evolution of polarization in such a fiber is of interest. There are probably many ways in which the Faraday effect can indicate the amount of current present. We shall consider the fiber geometry to be such that the electric current $I$ is parallel to the helical axis ($z$ axis) (Fig. 2). It is convenient to assume that the unit tangential vector of the right-handed helix is $\mathbf{s}_0$. It is obvious that the external optical activity (Faraday effect in radians) over an infinitesimal fiber segment $ds$ is $d\theta = -\mathbf{B} \cdot \mathbf{s}_0 V_d ds$, where $V_d$ stands for the Verdet constant with units of rad/[m(Wb/m$^2$)] (1/0.291 $\times$ 10$^3$ min/Gauss cm) whose positive value corresponds, by convention, to an $l$-rotatory optical activity. In addition, $B = \mu I/2R$ is the magnetic flux density measured in webers per square meter ($\mu = 4\pi \times 10^{-7}$ H/m in vacuum, $I$ is in amperes, and $R$ is in meters). Suppose that the coordinates of the fiber element are ($R \cos t$, $R \sin t$, $bt$) so that $\mathbf{s}_0 = 1/\sqrt{R^2 + b^2}(-R \sin t, R \cos t, b)$. On the other hand, the magnetic density flux vector $\mathbf{B}$ is seen to be $\mathbf{B} = B(-\sin t, \cos t, \phi)$. Expressions for optical activity $d\theta = \frac{1}{2}\delta_c' ds = (-BRV_d/\sqrt{R^2 + b^2})ds$ or $\delta_c' = -(2BRV_d/\sqrt{R^2 + b^2})$ are obtained. The expression is altered so that it is now positive for a left-handed helix in the same magnetic field. Together with a knowledge of the principal axes and the amount of stress-induced linear birefringence, this formula would imply that the parameters $P$ and $Q$ in Eqs. (7) are

$$P = \cos\lambda' s = \frac{j0.672 \times 10^6 R^2 r^2}{\lambda'(R^2 + b^2)^2} \sin\lambda' s,$$

$$Q = -\frac{b(1 - g)/(R^2 + b^2) - RBV_d/(\sqrt{R^2 + b^2})}{\lambda'} \sin\lambda' s,$$

$$\lambda' = \frac{1}{(R^2 + b^2)} \left\{ [b(1 - g) - RBV_d\sqrt{R^2 + b^2}]^2 + \left( \frac{0.672 \times 10^6 R^2 r^2}{R^2 + b^2} \right)^2 \right\}^{1/2}.$$

In particular, for a densely wound helix, $b \to 0$ (in which case the helix becomes a coil). If the coil is designed so that

$$\left| \frac{0.672 \times 10^6 r^2}{R^2} \right| \ll BV_d, \tag{11}$$

then $\lambda' = BV_d$, $P = \cos(BV_d s)$, and $Q = \sin(BV_d s)$. This describes a simple $l$-rotatory polarization with a rotating angle of $BV_d S$. This is the ideal situation in which the current sensor works accurately and linearly.[14] However, a

practical sensor may suffer from nonlinearity and inaccuracy because the light emerging from the sensor tends, in general, to be elliptically polarized when some linear birefringence is present, as is often the case.[14] The technique developed in this paper can effectively provide much insight into this problem since the output field is described thoroughly and the performance of the fiber sensor may be accurately estimated.

## CONCLUDING REMARKS

The polarization ellipse is uniquely determined by its plane-wave components. If the two transverse field components are normalized relative to either of these components, then the magnitude/phase ratio of the other can easily be determined by measuring the polarization ellipse. The relationship between the polarization ellipse (the ellipticity and inclined angle ratio) and the normalized field components is unique and is outlined first. It is the field that is the key parameter to the plane-wave evolution, even when the fiber itself suffers from a variation in the principal axes or in the hybrid birefringence rate along its length; an example is a general curvilinear fiber, in which polarization evolution has long been of interest. In this paper, the Jones matrix describing the electric field components of a plane wave has been generalized to include optical fibers that have distributed principal axes and linear and circular birefringence. The generalization can be made by means of mode coupling and field continuity. Only the latter approach is discussed in detail. This technique is obviously applicable to the popular twisted or spun fibers as well as to helical fibers that may have been exposed to external processes affecting optical activity, such as electric or magnetic fields and lateral pressures. A detailed description of the field of the output light is formulated individually for those fibers, and the results obtained are usually in good agreement with the experimental results and current theoretical analyses. The proposed matrix method, however, deals with general curvilinear fibers, and in this sense the method may be deemed to be a unified technique that should prove useful in practice.

## ACKNOWLEDGMENTS

The author wishes to thank W. A. Gambling and D. N. Payne for their leading roles in the research group. The author is also grateful to the reviewers for their helpful comments. R. Birch made the fiber detail of Ref. 26 available to the author, and R. Laming conducted the experiments. This research is sponsored by Science and Engineering Research Council, UK, and its support is sincerely acknowledged.

## REFERENCES

1. W. A. Shurcliff, *Polarized Light: Production and Use* (Harvard U. Press, Cambridge, Mass., 1962).
2. W. A. Shurcliff and S. S. Ballard, *Polarized Light* (Van Nostrand, Princeton, N.J. 1964).
3. R. C. Jones, "A new calculus for the treatment of optical systems," J. Opt. Soc. Am. **31,** 488–493, 493–499, 500–503 (1941).
4. R. C. Jones, "A new calculus for the treatment of optical systems," J. Opt. Soc. Am. **32,** 486–493 (1942).
5. R. C. Jones, "A new calculus for the treatment of optical systems," **37,** 107–112 (1947); **38,** 671–685 (1948).
6. A. Gerrard and J. M. Burch, *Introduction to Matrix Method in Optics* (Wiley, London, 1975).
7. E. Hecht and A. Jajac, *Optics* (Addison-Wesley, Reading, Mass. (1974), Chap. 8.
8. J. D. Kraus and K. R. Carver, *Electromagnetics*, 2nd ed. (McGraw-Hill, New York, 1973), Chaps. 10 and 11.
9. A. S. Marathay, "Matrix-operator description of the propagation of polarized light through cholesteric liquid crystals," J. Opt. Soc. Am. **61,** 1363–1372 (1971).
10. D. N. Payne, A. J. Barlow, and J. J. Ramskov Hansen, "Developments of low- and high-birefringence optical fibers," IEEE J. Quantum Electron. **QE-18,** 477–488 (1982).
11. W. J. Tabor and F. S. Chen, "Electromagnetic propagation through material possessing both Faraday rotation and birefringence: experiments with ytterbium orthoferrite," J. Appl. Phys. **40,** 2760–2765 (1969).
12. A. Papp and H. Harms, "Polarization optics of liquid-core fibers," Appl. Opt. **16,** 1315–1319 (1977).
13. H. Harms, A. Papp, and K. Kempter, "Magnetooptical properties of index-gradient optical fibers," Appl. Opt. **15,** 799–801 (1976).
14. S. C. Rashleigh and R. Ulrich, "Magneto-optic current sensing with birefringent fibers," Appl. Phys. Lett. **34,** 768–770 (1979).
15. R. Ulrich and A. Simon, "Polarization optics of twisted single-mode fibers," Appl. Opt. **18,** 2241–2251 (1979).
16. P. McIntyre and A. W. Snyder, "Light propagation in twisted anisotropic media: application to photoreceptors," J. Opt. Soc. Am. **68,** 149–157 (1978).
17. A. J. Barlow, "Birefringence in single-mode optical fibers," Ph.D. dissertation (University of Southampton, Southampton, UK, 1983).
18. M. Monerie and L. Jeunhomme, "Polarization mode coupling in long single-mode fibers," Opt. Quantum Electron. **12,** 449–461 (1980).
19. J. I. Sakai, S. Machida, and T. Kimura, "Existence of eigen polarization modes in anisotropic single-mode optical fibers," Opt. Lett. **6,** 496–498 (1981).
20. F. P. Kapron, N. F. Borrelli, and D. B. Keck, "Birefringence in dielectric optical waveguides," IEEE J. Quantum Electron. **QE-8,** 222–225 (1972).
21. G. H. Song and S. S. Choi, "Analysis of birefringence in single-mode fibers and theory for the backscattering measurement," J. Opt. Soc. Am. **2,** 167–170 (1985).
22. H. Takenaka, "A unified formulism for polarization optics by using group theory," Nouv. Rev. Opt. **4,** 37–41 (1973).
23. J. N. Ross, "The rotation of the polarization in low birefringence monomode optical fibers due to geometric effects," Opt. Quantum Electron. **16,** 455–461 (1984).
24. J. N. Ross, "Birefringence measurement in optical fibers by polarization—optical time-domain reflectometry," Appl. Opt. **21,** 3489–3495 (1982).
25. M. P. Varnham, R. D. Birch, and D. N. Payne, "Helical-core circularly birefringent fibers," in *Digest of the Fifth International Conference on Integrated Optics and Optical Fibre Communication, Eleventh Conference on Optical Communication* (Istituto Internazionale delle Comunicazioni, Genova, Italy, 1985), Vol. 1, pp. 135–138.
26. C. D. Hussey, R. D. Birch, and Y. Fujii, "Circularly birefringent single-mode optical fibers," Electron. Lett. **22,** 129–130 (1986).
27. R. Ulrich, S. C. Rashleigh, and W. Eickhoff, "Bending-induced birefringence in single-mode fibers," Opt. Lett. **5,** 273–275 (1980).
28. C. Y. H. Tsao and D. N. Payne, "Waveguide theory in curvilinear optical fiber such as helix," internal report (Department of Electronics, University of Southampton, Southampton, UK, 1986).
29. J. T. Cushing, *Applied Analytical Mathematics for the Physical Scientist* (Wiley, New York, 1975), Chap. 3.
30. B. Friedman, *Principles and Techniques of Applied Mathematics* (Chapman & Hall, New York, 1956), Chap. 2, p. 121.
31. L. Brand, *Vector and Tensor Analysis* (Wiley, New York, 1947), Chap. 3, pp. 105–108.